First Dredge-Up

Approximate solar compositions:

$$X(C^{12}) = 0.0030$$
$$X(C^{13}) = 3.7 \times 10^{-5}$$
$$X(N^{14}) = 0.0011$$
$$X(O^{16}) = 0.0096$$

NB X = mass fraction $= Y * A$

Y = mole fraction $= \frac{X}{A}$

A = mass number

By number: $C^{12}/C^{13} \simeq 90$

$C : N : O \simeq 3 : 1 : 8$

By mass: $Z = 0.02$ (closer to 0.017)

$Z_{CNO} = 0.7Z$
$= 0.014$

At dredge-up

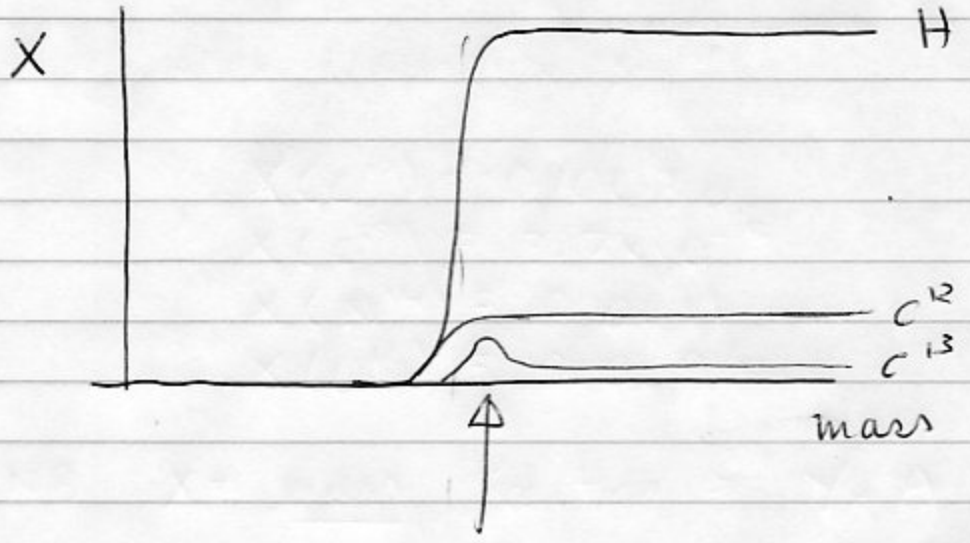

Small bump from C^{13} production.

C^{13} then in eq^{m} with C^{12}

$C^{12}/C^{13} \simeq 3$

But $C^{12} \to 0$ so $C^{13} \to 0$ also

core	envelope
X = 0	X = 0.7
Y = 0.98	Y = 0.28
Z = 0.02	Z = 0.02

(roughly)

NB Z is unchanged

Z_{CNO} is unchanged

But C, N (& maybe O) do change

Envelope : all have initial abunds

Interior : $C^{12} \simeq 0$

$N^{14} \simeq Z_{CNO}$

$C^{13} \simeq 0$ except for the small bump

$0.1 M_\odot$ to $0.01 M_\odot$ later

$$M(C^{13}) \text{ in bump} \simeq \frac{C^{12}}{3} \times 0.05 M_\odot$$

$$\simeq 5 \times 10^{-5} M_\odot$$

$O^{16} \simeq 0$ ($O^{16} \rightarrow N^{14}$ in shell)

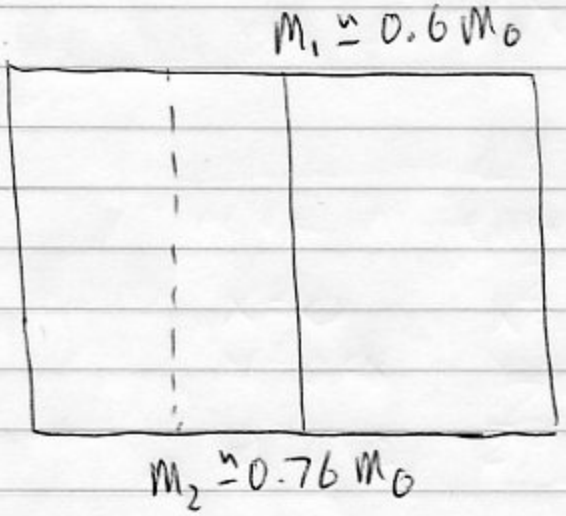

$\Delta M \simeq 0.16 M_\odot$

initial : subscript 0

interior : subscript i

final : no subscript

C^{12} By mass conservation:

$$M_2 C^{12} = M_1 C_0^{12} + \Delta M C_i^{12}$$

$$C^{12} = \frac{M_1 C_0^{12}}{M_2}$$

$$= 0.6 \times 0.003 / 0.76$$

$$= 0.0024$$

C^{13} $M_2 C^{13} = M_1 C_0^{13}$ + bump content

$$C^{13} = \frac{0.6 \times 3.7 \times 10^{-5} + 5 \times 10^{-5}}{0.76}$$

$$= 9.5 \times 10^{-5}$$

N^{14} $M_2 N^{14} = M_1 N_0^{14} + \Delta M N_i^{14}$

$$= 0.6 \times 0.0011 + 0.16 \times 0.014$$

$$N^{14} = 3.8 \times 10^{-3}$$

etc.

So by number $\frac{C^{12}}{C^{13}} = \frac{0.0024}{12} / \frac{9.8 \times 10^{-5}}{13}$

$= 26$ (from 90!)

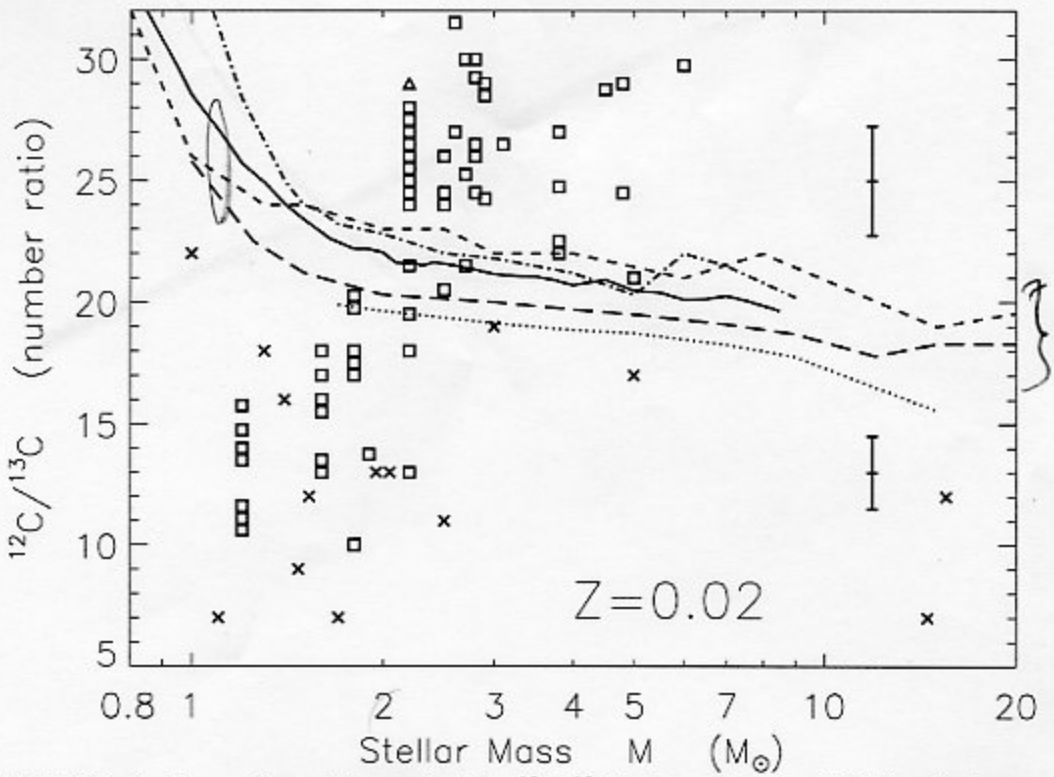

FIGURE 4. Comparison of observed stellar $^{12}C/^{13}C$ ratios with theoretical first dredge-up predictions of various authors (for stars of solar metallicity). *Squares*: galactic open cluster observations [23] (error-bars at right of plot show typical observational error; *triangle* indicates lower limit), having accurate determinations of the stellar mass. *Crosses*: isolated star observations [26,27,30], with masses uncertain by a factor of ~ 2. Theoretical curves: *solid*: Boothroyd & Sackmann [5], *dotted*: El Eid [18], *short-dashed*: Dearborn [15], *long-dashed*: Schaller *et al.* [60] and also Charbonnel [13], *dot-dashed*: Bressan *et al.* [9].

In Figure 5, the solid lines show theoretical predictions of the $^{12}C/^{13}C$ ratio resulting from first dredge-up, as a function of stellar mass and metallicity. The trend with stellar mass is due to the fact that low mass stars have narrower ^{13}C-pockets than intermediate mass stars (the entire ^{13}C-pocket is always dredged up). The trend of increased $^{12}C/^{13}C$ ratio for reduced metallicity Z is due to the fact that the initial stellar $^{12}C/^{13}C$ ratio was assumed to be inversely proportional to Fe/H [67,68]; models where the initial stellar $^{12}C/^{13}C$ ratio was assumed to be independent of metallicity show a very small trend in the opposite direction (see also Charbonnel [13]). The average observed $^{12}C/^{13}C$ ratios in RGB and post-RGB stars, in galactic open clusters of near-solar metallicity, are shown by the open circles in Figure 5; for stars of mass $> 2M_\odot$, they are in reasonable agreement with the theoretical curves, (although they suggest that the ^{13}C-pocket may in fact be about 20% smaller than predicted by standard theoretical models). For stars of mass $\lesssim 2\,M_\odot$, the observations

This again alters the surface compositions of ^{4}He, ^{12}C, ^{13}C, and ^{14}N, and actually reduces the mass of the H-exhausted core, because in the process of mixing ^{4}He outward we also mix H inward (see inset (e) in Figure 2). Note that there is a critical mass (of about $4M_\odot$, but dependent on composition) below which the second dredge-up does not occur. Following second dredge-up, the H-shell is re-ignited, and the first thermal pulse occurs soon after: the star has reached the thermally-pulsing AGB, or TP-AGB. Note that at this stage the structure is qualitatively similar for all masses.

C The Key Mixing Events

As we saw above, when a star approaches the RGB after the completion of main sequence core hydrogen burning, its convective envelope deepens, eventually dredging up products of main sequence nucleosynthesis (*first dredge-up*). The first dredge-up ceases when the convective envelope reaches its maximum inward penetration, and then begins to recede again. This leaves behind a sharp composition discontinuity. For low mass stars ($\lesssim 2.5M_\odot$), the hydrogen-burning shell catches up to and erases this discontinuity while the star is still on the RGB; for higher masses ($\gtrsim 2.5\ M_\odot$), the star leaves the RGB before this can take place. There is observational evidence from surface abundance changes on the RGB [23,24,30,43,38,37,13,61] that, once the composition discontinuity is erased, some form of non-convective "*extra mixing*" takes place, which transports material from the (relatively cool) bottom of the convective envelope down close to the hydrogen-burning shell (where nuclear burning can alter its composition) and then up to be mixed back into the convective envelope. Boothroyd, Sackmann, & Wasserburg [8] referred to this process as "*cool bottom processing*"; the precise mixing mechanism is not well understood, but is frequently assumed to be rotation-induced, e.g., meridional circulation [66] or shear-induced turbulence [14] (similar to the extra mixing process on the main sequence that yields the large ^{7}Li-depletions in $\sim 1\ M_\odot$ main sequence stars [70,52]). Note that "extra mixing" or "extra deep mixing" generally result in "cool bottom processing" and hence in surface abundance changes; these three terms are used essentially synonymously hereafter.

Low mass stars experience significant mass loss on the RGB (totaling $\sim 0.2M_\odot$), with peak mass loss rates of $\dot{M} \sim 10^{-7}M_\odot$/yr near the tip of the RGB; some grain formation may take place during this stage.

After the completion of core helium burning, helium burns in a shell surrounding the degenerate carbon–oxygen core; the star ascends the AGB, and the convective envelope deepens again. In intermediate mass stars, the hydrogen-burning shell is temporarily extinguished and envelope convection reaches into and below the position of the hydrogen-burning shell, bringing more nucleosynthesized material to the surface (*second dredge-up*). This occurs on the early AGB (E-AGB). Shortly thereafter, as the helium shell

approaches the hydrogen shell, the hydrogen shell re-ignites, and periodic nuclear runaway events occur in the helium-burning shell (called thermal pulses or helium shell flashes); this stage of evolution is called the thermally-pulsing AGB (TP-AGB), and is discussed in more detail in section IV below. The strong nuclear energy generation in these thermal pulses causes a convective region to grow outwards from the helium-burning shell, mixing the products of partial helium burning outwards almost to the base of the hydrogen-burning shell. The energy input causes the star to expand and cool, turning off the thermal pulse and weakening or extinguishing the hydrogen-burning shell; the convective envelope is thus able temporarily to reach into the intershell region where the products of helium burning were deposited and mix them to the surface in what is known as the *third dredge-up* (see section V). Note that the third dredge-up is a repeating phenomenon, occurring after almost each pulse (except for the first few) in each TP-AGB star. This is in contrast to the first and second dredge-up events, which occur at most once per star (low mass stars do not experience the second dredge-up at all).

In stars with masses $\gtrsim 4\,M_\odot$, the convective envelope is deep enough during the long interpulse periods that it reaches into the hydrogen-burning shell, i.e., nuclear processing takes place at the bottom of the convective envelope, altering its composition. This is known as "*hot bottom burning*", and is discussed more fully in section VI.

The AGB stage of evolution is terminated when mass loss has removed almost all of the star's envelope (the "planetary nebula" stage follows). In the "superwind" which terminates the AGB, mass loss rates of $\dot{M} \sim 10^{-4}\,M_\odot$/yr are observed; such relatively dense outflows from cool stars are favorable sites for grain formation.

III THE RGB AND E-AGB: FIRST AND SECOND DREDGE-UP, AND EXTRA MIXING

Theoretical models of first and second dredge-up without any "extra mixing" or "cool bottom processing" [15,60,9,13,18,5] agree with each other reasonably well (see, e.g., Fig. 4); results presented here are from the models of Boothroyd & Sackmann [4,56,57,5]. For solar metallicity ($Z = 0.02$), solar elemental and isotopic abundances were assumed to represent the initial stellar composition. The α-element enhancement at lower metallicity was approximated by setting [O/Fe] $= -0.5$ [Fe/H] for [Fe/H] > -1, and constant [O/Fe] $= +0.5$ for [Fe/H] ≤ -1; [C/Fe] and [N/Fe] were taken to be independent of metallicity, as indicated by observations (see Timmes *et al.* [68], and references therein). The initial isotopic ratios ^{12}C/^{13}C, ^{16}O/^{17}O, and ^{16}O/^{18}O were taken to be inversely proportional to Fe/H, as suggested by the galactic chemical evolution models of Timmes *et al.* [68,67] (there are few observational constraints on the evolution of these isotopic ratios in the interstellar

medium). Nuclear rates from Caughlan & Fowler [12] were used, except for $^{12}C(\alpha,\gamma)$ (where the rate was multiplied by 1.7, as recommended by Weaver & Woosley [72]), and $^{17}O(p,\alpha)$ and $^{17}O(p,\gamma)$, where the 1990 rates of Landré *et al.* [40] or the (slightly higher) 1995 rates of Blackmon *et al.* [2,1] were used. A value of the mixing length to pressure scale height ratio of $\alpha = 2.1$ was required in order to obtain a correct model of the Sun [56,57] (note that the value of α has almost no effect on the depth of dredge-up, as has already been noted by Charbonnel [13]). Reimers-formula red giant mass loss [53,39,5] had negligible effect, as very little mass had been lost at the time of first dredge-up (or at the time of second dredge-up, in intermediate mass stars).

Models of "extra mixing" and the consequent cool bottom processing on the RGB [66,14,71,17,5,55] generally contain free parameter(s) to control the depth and/or speed of the mixing, whose values may be determined by matching observed RGB stellar compositions. Models presented in this work [71,5,55] use a simple "conveyor-belt" circulation scenario, where the extra mixing reaches down into the outer wing of the hydrogen-burning shell. The temperature difference $\Delta \log T$ between the bottom of mixing and the bottom of the hydrogen-burning shell was considered a free parameter (with a value $\Delta \log T \approx 0.26$ obtained by requiring that a $Z = 0.02$, 1.2 $M_\odot$ case reproduce the average observed $^{12}C/^{13}C$ ratio). Changes in the envelope structure were followed as the star climbs the RGB, by using the structure from a stellar evolutionary run without extra mixing (as the effect of the extra mixing on the envelope structure should be small). For carbon and heavier elements, the speed of circulation is irrelevant within wide limits (a larger number of rapid circulation passes has the same effect as a smaller number of slow ones).

During core hydrogen burning on the main sequence, partial hydrogen burning in the outer part of the core produces a region of altered elemental and isotopic abundances; as the star approaches the RGB and a deep convective envelope develops, this region is engulfed and mixed into the envelope. Lithium, beryllium, and boron have been destroyed in all but the outer layers of the star. Partial *p-p* chain burning has left behind a pocket rich in ^{3}He. Slightly further in, a large ^{13}C-pocket exists, where $^{12}C/^{13}C$ approaches its nuclear equilibrium ratio of ~ 3, but only part of the ^{12}C has been burned. Below this ^{13}C-pocket, both ^{12}C and ^{13}C have been almost completely converted into ^{14}N, and most of the ^{15}N and ^{18}O have been destroyed; in this region, ^{17}O begins to be enhanced, from partial burning of ^{16}O. These composition profiles are shown in Figure 3.

As the ^{13}C-pocket is engulfed by the convective envelope, the surface $^{12}C/^{13}C$ ratio is reduced from its large initial value (about 90 for Solar compositions) to ~ 30 in low mass stars and somewhat less (~ 20) in intermediate mass stars (see theoretical curves of Fig. 4). However, observations of RGB and post-RGB $^{12}C/^{13}C$ ratios in galactic open clusters [23] indicated the opposite trend with stellar mass (see Fig. 4).

Gilroy & Brown [24] observed $^{12}C/^{13}C$ ratios as a function of luminosity on

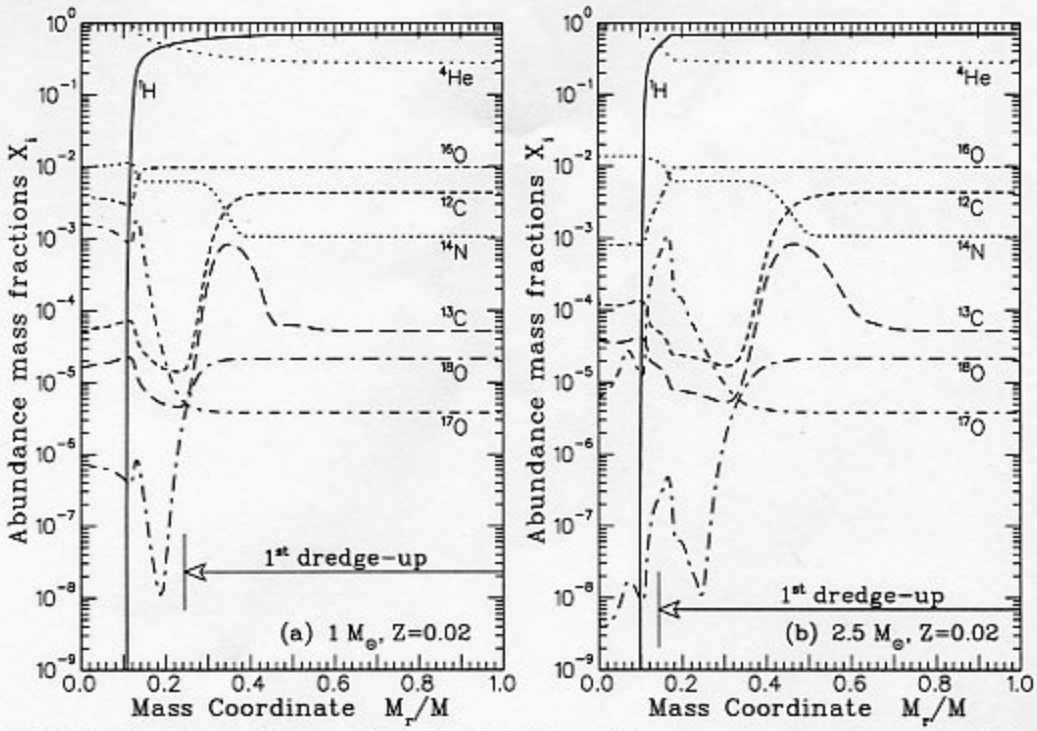

FIGURE 3. Composition profiles as a function of the normalized mass coordinate, for stars near the base of the RGB (prior to first dredge-up); the depth later reached by first dredge-up is indicated by the horizontal arrow at the bottom. (*a*) 1.0 $M_\odot$ star, (*b*) 2.5 $M_\odot$ star; both with solar metallicity ($Z = 0.02$).

the RGB. They found that observed and theoretical ratios agree very well up to and somewhat past the point of deepest first dredge-up, but that excess ^{13}C began to appear after the point (somewhat higher on the RGB) where the hydrogen-burning shell reached the composition discontinuity that was left behind by deepest first dredge-up. As discussed by Charbonnel [13], this is consistent with cool bottom processing that is due to relatively slow (weak) extra mixing, because the mixing instability can be stabilized by a molecular weight gradient. The large molecular weight gradient at the composition discontinuity acts as a barrier to mixing, preventing envelope material from being transported down near the hydrogen-burning shell. Once the hydrogen-burning shell has reached (and erased) the composition discontinuity, the extra mixing can transport envelope material down into the outer wing of the hydrogen-burning shell, where hydrogen-burning produces a molecular weight gradient (how deep into the shell the mixing would reach is determined by the unknown details of the mixing mechanism, but can be estimated by the observed nucleosynthetic results at the stellar surface). For stars with masses $> 2\,M_\odot$, the end of the RGB occurs before the composition discontinuity has been erased; thus these intermediate-mass stars do not encounter RGB cool bottom processing.

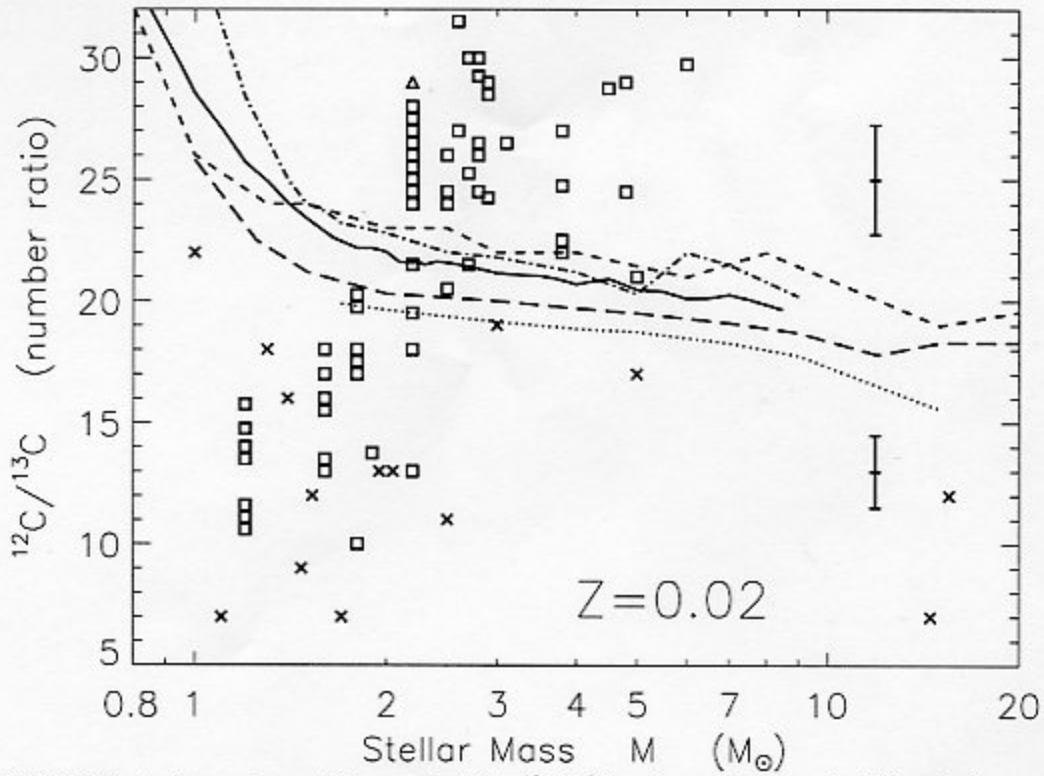

FIGURE 4. Comparison of observed stellar $^{12}C/^{13}C$ ratios with theoretical first dredge-up predictions of various authors (for stars of solar metallicity). *Squares*: galactic open cluster observations [23] (error-bars at right of plot show typical observational error; *triangle* indicates lower limit), having accurate determinations of the stellar mass. *Crosses*: isolated star observations [26,27,30], with masses uncertain by a factor of ~ 2. Theoretical curves: *solid*: Boothroyd & Sackmann [5], *dotted*: El Eid [18], *short-dashed*: Dearborn [15], *long-dashed*: Schaller *et al.* [60] and also Charbonnel [13], *dot-dashed*: Bressan *et al.* [9].

In Figure 5, the solid lines show theoretical predictions of the $^{12}C/^{13}C$ ratio resulting from first dredge-up, as a function of stellar mass and metallicity. The trend with stellar mass is due to the fact that low mass stars have narrower ^{13}C-pockets than intermediate mass stars (the entire ^{13}C-pocket is always dredged up). The trend of increased $^{12}C/^{13}C$ ratio for reduced metallicity Z is due to the fact that the initial stellar $^{12}C/^{13}C$ ratio was assumed to be inversely proportional to Fe/H [67,68]; models where the initial stellar $^{12}C/^{13}C$ ratio was assumed to be independent of metallicity show a very small trend in the opposite direction (see also Charbonnel [13]). The average observed $^{12}C/^{13}C$ ratios in RGB and post-RGB stars, in galactic open clusters of near-solar metallicity, are shown by the open circles in Figure 5; for stars of mass $> 2M_\odot$, they are in reasonable agreement with the theoretical curves, (although they suggest that the ^{13}C-pocket may in fact be about 20% smaller than predicted by standard theoretical models). For stars of mass $\lesssim 2\ M_\odot$, the observations

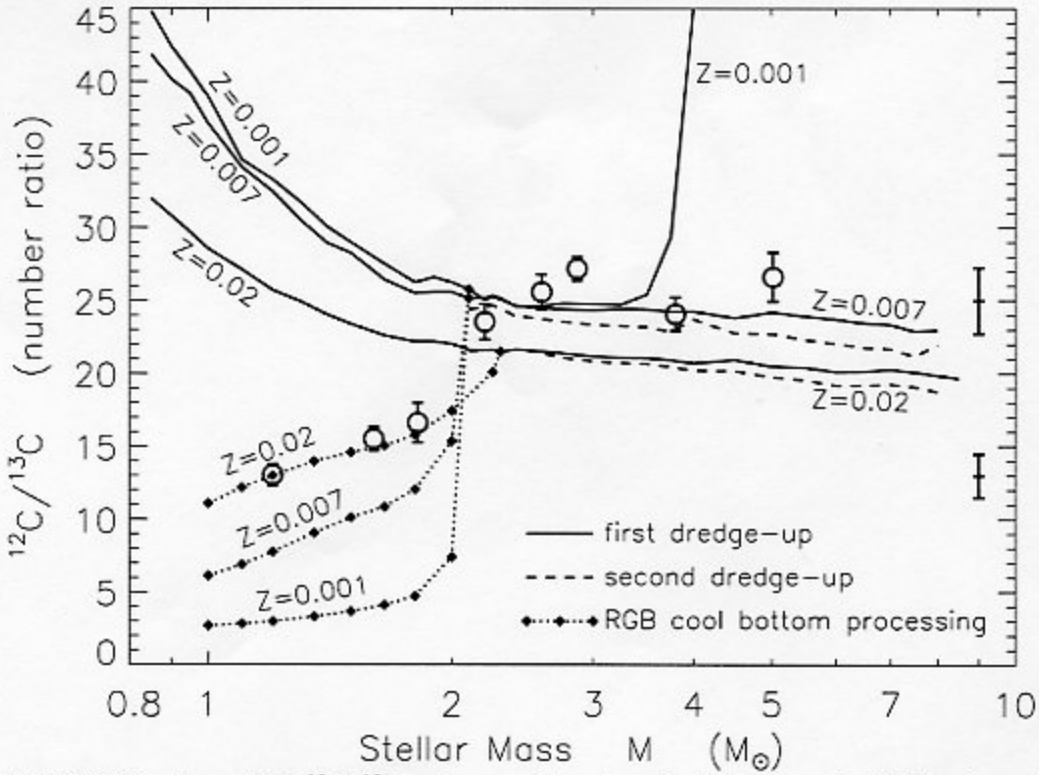

FIGURE 5. Theoretical $^{12}C/^{13}C$ ratios resulting from first dredge-up (*solid lines*), cool bottom processing on the RGB (*diamonds*), and second dredge-up on the E-AGB in intermediate-mass stars (*dashed lines*), for three metallicities Z (for clarity, second dredge-up is not plotted for $Z = 0.001$; it coincides approximately with the $Z = 0.007$ case.) Initial stellar $^{12}C/^{13}C$ ratios were assumed to be inversely proportional to Fe/H, as per galactic chemical evolution models of Timmes *et al.* [67,68]. *Open circles* show average ratio from galactic open cluster observations [23], with error-bars showing internal statistical error in the mean (from observational scatter); error-bars at far right show typical observational errors. Note cool bottom processing models were normalized at 1.2 $M_\odot$ (for $Z = 0.02$).

reflect the "extra mixing" and cool bottom processing that produces additional ^{13}C subsequent to first dredge-up. Estimates of the $^{12}C/^{13}C$ ratio at the tip of the RGB that result from cool bottom processing, with the simple circulation model described above, are shown by the solid diamonds in Figure 5. The depth of the extra mixing in the models is determined by the observed $^{12}C/^{13}C$ ratio in stars of mass $1.2M_\odot$, and thus by definition the cool bottom processing models reproduce that observational point; however, they also reproduce the trend with stellar mass shown by the observations of stars with masses between 1.2 and 2 $M_\odot$. Under the assumption that extra mixing always reaches the same point in the outer wing of the hydrogen-burning shell, independent of metallicity, one finds, as shown in Figure 5, that cool bottom processing has a much greater effect on low metallicity (Population II) stars than in stars of

O^{16}

$$M_2 O^{16} = M_1 O^{16}_{0} + \Delta M . O^{16}_{i}$$

$$O^{16} = \frac{0.6 \times 0.0096 + 0}{0.72}$$

$$\simeq 0.008$$

So initially C^{12}/O^{16} by number $= \frac{0.0030}{12} / \frac{0.0096}{16}$

$$= 0.42$$

After FDU: $\frac{C^{12}}{O^{16}} = \frac{0.0024}{12} / \frac{0.008}{16}$

$$= 0.40$$

Slightly lower – not much change!